LUND UNIVERSITY

Particulate PAH Emissions from Residential Biomass Combustion: Time-Resolved Analysis with Aerosol Mass Spectrometry

Eriksson, Axel; Nordin, Erik; Nystrom, R.; Pettersson, E.; Swietlicki, Erik; Bergvall, C.; Westerholm, R.; Boman, C.; Pagels, Joakim

Link to publication

Particulate PAH Emissions from Residential Biomass Combustion: Time-Resolved Analysis with Aerosol Mass Spectrometry

A. C. Eriksson,*,[†] E. Z. Nordin,[‡] R. Nyström,[§] E. Pettersson,[§] E. Swietlicki,[†] C. Bergvall,[∥] R. Westerholm,[∥] C. Boman,[§] and J. H. Pagels[‡]

[†]Nuclear Physics, Lund University, P.O. Box 118, SE-22100, Lund, Sweden

[‡]Ergonomics and Aerosol Technology, Lund University, P.O. Box 118 SE-22100, Lund, Sweden

[§]Thermochemical Energy Conversion Laboratory, Department of Applied Physics and Electronics, Umeå University SE-90187, Umeå, Sweden

[∥]Department of Analytical Chemistry, Arrhenius Laboratory, Stockholm University SE-10691 Stockholm, Sweden

S *Supporting Information*

ABSTRACT: Time-resolved emissions of particulate polycyclic aromatic hydrocarbons (PAHs) and total organic particulate matter (OA) from a wood log stove and an adjusted pellet stove were investigated with high-resolution time-of-flight aerosol mass spectrometry (AMS). The highest OA emissions were found during the addition of log wood on glowing embers, that is, slow burning pyrolysis conditions. These emissions contained about 1% PAHs (of OA). The highest PAH emissions were found during fast burning under hot air starved combustion conditions, in both stoves. In the latter case, PAHs contributed up to 40% of OA, likely due to thermal degradation of other condensable species. The distribution of PAHs was also shifted toward larger molecules in these emissions. AMS signals attributed to PAHs were found at molecular weights up to 600 Da. The vacuum aerodynamic size distribution was found to be bimodal with a smaller mode ($D_{va} \sim 200$ nm) dominating under hot air starved combustion and a larger sized mode dominating under slow burning pyrolysis ($D_{va} \sim 600$ nm). Simultaneous reduction of PAHs, OA and total particulate matter from residential biomass combustion may prove to be a challenge for environmental legislation efforts as these classes of emissions are elevated at different combustion conditions.
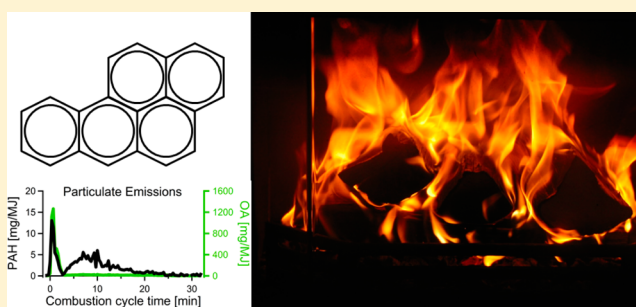
INTRODUCTION

Biomass combustion is widely used globally for energy production, domestic heating and cooking. Due to the low net emissions of greenhouse gases there is an increasing interest in further extending the share of biomass for energy production. However, particulate air pollution from wood combustion has been associated with health effects in the population.[1−3] Wood combustion PM has been suggested to be at least as toxic as other sources on a mass basis.[4] A major reason for that is presumably the organic fraction, including for example polycyclic aromatic hydrocarbons (PAHs).[5] Benzo(a)pyrene (BaP, a five ring particle phase PAH) is classified as a human carcinogen.[6] Measurements in regions with dense use of wood stoves and fireplaces have shown elevated levels of PAHs in ambient air.[7] Laboratory studies have confirmed that the aerosol emissions, particularly at high burn rates, contain high levels of PAHs.[8−10] PAHs emitted from biomass combustion span a range of volatilites.[11] Those with two to three benzene rings are predominantly found in the gas phase, while molecules with five rings or more predominantly occur in the particle phase at atmospheric conditions.[12]

Gas chromatography−mass spectrometry (GC-MS) has proven to be an excellent tool with low detection limits for speciated quantification of particle and gas phase PAHs for averages over full combustion cycles.[9,12,13] However, the time resolution of such off-line methods is limited, impeding mechanistic understanding of PAH formation and emissions in batch-wise wood combustion systems. Heringa et al.[14] recently provided detailed highly time-resolved data on organic emissions from residential wood combustion using high-resolution time-of flight aerosol mass spectrometry (AMS). However, in that study PAHs were not included in the analysis.

PAHs undergo relatively little fragmentation during vaporization and ionization in the AMS, which enables quantitative measurements of the concentration of PAHs separated into groups by molecular weight.[15,16] However, separation of PAH isomers is not possible through AMS. Comparisons between quadrupole AMS (Q-AMS) and filter samples analyzed with

GC-MS show that the AMS can be used to quantify particulate PAHs in a polluted environment using a simple procedure to subtract non-PAH organic signals at the PAH peaks.[15] Poulain et al.[7] found good agreement between particulate PAHs derived from AMS and GC-MS in ambient measurements influenced by wood combustion. Weimer et al.[17] used a Q-AMS to investigate time-resolved organic emissions from a wood stove and noted highly variable particulate PAH emissions. A recent study by Elsasser et al.[18] confirmed the capability of AMS to characterize dynamic changes in particulate emission, including variations in PAH fraction. Neither study investigated the combustion conditions resulting in high PAH emissions systematically.

In this study we combined highly time-resolved PAH measurements using AMS and combustion gas emission measurements on a conventional wood stove and an adjusted pellet stove. The aim was to investigate the influence of burn rate and combustion phase on emissions of PAHs and OA.

■ MATERIALS AND METHODS

Combustion Facilities. A conventional natural draft wood stove that was extensively sold on the Swedish market during the 1990s was used in this study.[9] The wood stove was operated in a laboratory flue gas setup that enables controlled combustion and sampling conditions. A flue gas fan was used to create a (relevant) chimney draft resulting in a constant air flow into the stove over the combustion cycle. This improved the repeatability of the burning cycles and simplified the data reduction to derive useful emission measures (mg/MJ and μg/s). The stove was operated in two modes: nominal burn rate (NB), and high burn rate (HB). For HB 2.9 kg fuel (dry mass) was combusted per hour, compared to 1.9 kg/h for NB. The logs were also smaller and the cycle duration was shorter in HB, as further described in the Supporting Information (SI).

Full combustion cycles were investigated starting with the addition of fuel on glowing embers. For both operating modes, each combustion cycle was separated into three phases: fuel addition, intermediate, and burn out as described in the SI. In addition, a fourth experimental phase was investigated, in which further fuel addition was performed during the (flaming) intermediate phase at HB. We note that the assignment of phases to a combustion cycle is an idealization, since the phase of a batch of fuel is not synchronized, as illustrated by Elsasser et al.[18] However, given the emission patterns observed (see Figures 1 and 2), dominant phases were assigned to the combustion cycles as described above. The initial cold start at each experiment (i.e., kindling phase) was not included in this study.

The emissions from this type of wood stove for different fuel and operation parameters were previously extensively characterized for full cycle PM, PAH and volatile organic compound speciation and concentrations as well as online particle size distributions.[9]

The pellet stove was a prototype of a commercial stove that was adjusted technically to enable operation in two specific combustion modes: "optimal" and "reduced air supply". The reduced air supply mode was not intended to represent realistic emissions from pellet stoves. The purpose was to produce controlled generation of PAH rich particles in this appliance. The wood stove experiments by contrast were designed to emulate realistic user behavior.

The wood stove was fueled with Birch logs, while the pellets were made from a mixture of Pine and Spruce. SI Table S1

contains further information about fuel characteristics. Table 1 lists the range of flue gas mixing ratios and heat release rates of

Table 1. Average (Range) Flue Gas Composition and Heat Release Rates for the Different Operating Conditions of the Stoves; Wood Stove Data from the Intermediate Phase

	O_2 [%]	CO [ppm]	heat release rate [kW]
wood stove, nominal burn rate (NB): 1.9 kg/h	11 (7−14)	1300 (520−5600)	12 (9−17)
wood stove, high burn rate (HB): 2.9 kg/h	5 (2−14)	9100 (920−19000)	25 (12−29)
pellet stove, optimal	11 (7−14)	186 (20−850)	4 (4−5)
pellet stove, reduced air supply	4 (2−7)	4100 (730−16000)	2 (2−3)

the investigated combustion conditions. Note that heat release refers to heat output from the chemistry of the combustion, not heat transferred to the building which is beyond the scope of this work.

Aerosol Sampling and Instrumentation. The sampling was carried out from a flue gas temperature of 100−300 °C (dependent on appliance used and combustion conditions). The primary dilution was achieved by a porous tube diluter,[19] operated with filtered dilution air at ambient temperature followed by one or two ejector diluters coupled in series. The total dilution ratio (300−3000) was adjusted so that average organic mass loadings during the intermediate phase were between 5 and 15 μg/m³ for both wood stove modes and for reduced air supply to the pellet stove. These mass loadings are relevant for atmospheric conditions, which is important due to the controlling effect of concentration on gas/condensed phase partitioning.[20] Carbon monoxide, nitrogen oxides and oxygen concentrations in the undiluted flue gases were analyzed by electrochemical sensors with a flue gas analyzer (model 350XL, TESTO, Germany). The setup including filter sampling and analysis is further described in SI.

The size-resolved particulate chemical composition was measured in situ by AMS.[21] The technique involves sampling of the particles directly after flue gas dilution into a vacuum system, flash vaporization at 600 °C, 70 eV electron ionization and time-of flight mass spectrometry. We report the total organic particulate matter (OA) and the subcategory PAHs. PAHs were derived from signals originating from unfragmented or nearly unfragmented PAHs, referred to as PAH marker signals (illustrated in Figure 4 and SI Figure S3). We used a modified version of the parametrization proposed by Dzepina to quantify the concentrations of PAH.[15] AMS operation and data reduction is further described in the SI.

Calculation of Time-Resolved Emissions. In order to adequately compare different modes of operation and combustion appliances, the measured flue gas and PM concentrations were converted into emissions, in mg/s and mg/MJ, through eqs 1−3 below. The total heat release Q_{tot} [MJ] in a full batch was calculated from the dry mass of fuel added m_{tot} [kg] and the lower heating value HV_{fuel} [MJ/kg] measured through calorimetry:

$$Q_{tot} = m_{tot} \times HV_{fuel} \tag{1}$$

We used a simplified version of the oxygen consumption method[22] to calculate the heat release over time. This is henceforth referred to as heat release rate (kW). The method

utilizes the fact that biomass combustion consumes approximately one mole of O_2 per 420 kJ of heat released, independent of the changes in fuel composition that occurs over the combustion cycle.[22] A flue gas fan was used to accomplish a constant flow into the stove; hence, the decrease in oxygen concentration was proportional to reaction rate. Accordingly, the heat release Q_i [MJ] at each time step i was calculated:

$$Q_i = \frac{20.9 - O_2(i)}{\sum_i (20.9 - O_2(i))} \times Q_{tot} = \frac{\Delta O_2(i)}{\sum_i \Delta O_2(i)} \times Q_{tot}$$

(2)

From the time-resolved mass concentrations, C [mg/m³], (accounting for dilution), duration of a time step, t [s], and volumetric total flow rate, flow [m³/s at STP], emissions, E [mg/MJ], were calculated:

$$E_i = \frac{e_i}{Q_i} = \frac{C_i \times flow \times t}{Q_i}$$

(3)

In [3], e_i is the emitted mass of pollutants in mg over a time interval, i. The volumetric flow of air into the stove was inferred from the measured flue gas O_2 concentration by relating $\sum_i \Delta O_2(i)$ to the number of moles of reacted O_2 required to produce Q_{tot}. The calculations and their associated uncertainties are further discussed in the SI.

■ RESULTS AND DISCUSSION

Time-Resolved Emissions of Particle Phase PAHs and Organics from the Wood Stove. The measured particulate organic and PAH concentrations varied considerably over the combustion cycle of a batch of wood logs. Figure 1 shows representative nominal and high burn rate wood stove experiments. Based on the observed temporal variability, the cycles were divided into three phases: (i) "fuel addition", which starts when fuel is added on the glowing embers of the preceding cycle and lasts until the flue gas O_2 content drops below 9%, (ii) "intermediate" phase, that follows after the initial fuel addition phase and includes the whole continuous flaming phase, and finally (iii) the "burn out" phase, starting when the O_2 content rises above 14% (see SI). The top panel of Figure 1 displays the measured mass concentrations of PAHs and OA (accounting for dilution). Note that due to the constant flow rate through the stove, emissions in µg/s are proportional to these measured mass concentrations. The middle panel shows the commonly used modified combustion efficiency (MCE), defined as the ratio between CO_2 and (CO_2+CO) produced.

By far, the highest emissions of OA in µg/s were found for the addition of fuel on glowing embers. In the intermediate and burn out phases, considerably lower OA emission rates were found. PAHs showed a different emission profile from OA, with elevated emissions during: (i) fast burning (heat release rate >23 kW) in the intermediate phase of HB experiments when O_2 drops below 5%, CO emissions are elevated and MCE reduced, and (ii) slow burning (heat release rate <10 kW) following addition of wood logs on glowing embers (in both NB and HB experiments). The burn out phase was associated with low emissions of both OA and particulate PAHs.

Figure 2 shows the average emissions of OA and PAHs observed in nominal (NB) and high (HB) burn rate experiments. The top panel displays the emissions in mg integrated over time for each combustion phase and the full cycle. In the NB experiments, most of the OA (~80%) was emitted during the fuel addition phase. The amount of OA, and PAH fraction, during fuel addition was similar for NB and HB. In the nominal burn rate experiments, about half of the PAH emission occurred in the intermediate phase. For high burn rate cycles, the PAH emissions were significantly higher (about an order of magnitude) than for NB, due to very high PAH emissions in the intermediate phase. This was caused by the occurrence of fast burning conditions illustrated in Figure 1.

The full batch particle phase PAH emissions were 0.1 mg/MJ (1.5 mg/kg) for NB and 0.7 mg/MJ (13 mg/kg). The middle panel of Figure 2 illustrates that the emissions expressed per MJ are very high during fuel addition, while this phase contributes less to the total emissions (mg).

Controlled Combustion in Pellet Stove. For the controlled combustion in the pellet stove, two cases were investigated. During efficient "optimized" combustion, the PAH emissions were low, <0.1 mg/MJ (<2 mg/kg dry fuel). The emissions of OA were also low, ~0.5 mg/MJ. In this case the PM is strongly dominated by inorganic components such as potassium sulfates and chlorides (PMtot ~ 20 mg/MJ).[23,24] Air starved combustion conditions were investigated by lowering the air supply to the combustion unit until an operation mode: "reduced air supply", with intermittent air starved situations was achieved. For this combustion case (SI Figure S6), elevated PAH and OA emissions were observed, about 0.5 mg/MJ (10 mg/kg dry fuel) and ~1.5 mg/MJ, respectively, which coincided with peaks in CO. Thus, using artificially degraded pellet combustion we were able to under controlled conditions produce PAH rich aerosols that can be used in toxicological studies and for collection of material for off-line analysis where more stable conditions are desirable.

Relationship between PAH Emissions and Combustion Conditions. To further investigate the strongly elevated PAH emissions during fast burning conditions, a small batch (0.8 kg) of additional fuel was added twice in the later parts of the intermediate (flaming) phase in a HB experiment (SI Figure S4). This procedure resulted in fuel rich conditions at high temperatures with O_2 levels in the flue gases <2% (i.e., the highest heat release rates in the study, about 28 kW). These conditions resulted in very high PAH emissions (up to 8 mg/MJ). Under these conditions, the PAH fraction of the OA peaked at 40% while the increase in OA was moderate.

We investigated relationships between emitted particulate PAHs, the heat release rate and simple-to-measure flue gases, such as O_2 and CO. We found that PAH emissions per heat released were low to moderate (<0.4 mg/MJ) at excess O_2 concentrations between 5 and 12%, but elevated under slow burning pyrolysis conditions upon addition of fuel and particularly at fast burning with hot air starved conditions (Figure 3). We also found correlations between CO and PAH emissions (not shown) for a given combustion phase, but it was clear that CO can not be used as a general tracer for particulate PAHs in time-resolved analysis. For example, the burn out phases resulted in relatively high CO emissions (and consequently a low MCE) but low PAH emissions.

PAH Carbon Number Distributions. Figure 4 displays normalized OA mass spectra recorded during the intermediate phase of a high burn rate wood stove combustion cycle (top), and reduced air supply pellet stove operation (bottom). PAH markers contributed 12% of the signal in the pellet case and 8% for the wood stove; the estimated PAH mass fractions were 22% and 14%, respectively (see SI). Due to the heavy fragmentation of non-PAH molecules, their contribution
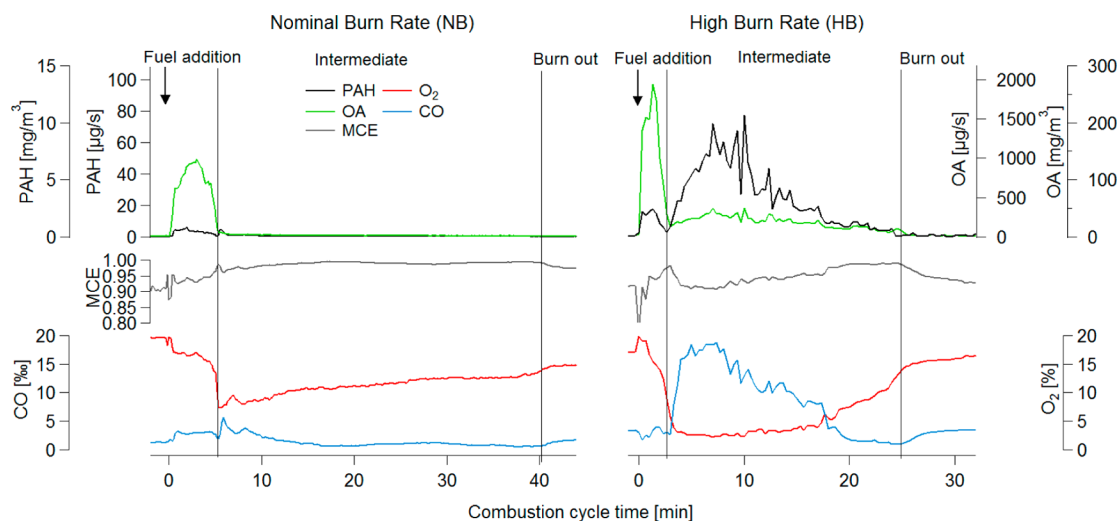
Figure 1. Time series of PAH and OA emissions from nominal (left), and high (right) burn rate wood stove experiments. $t = 0$ marks the start of a combustion cycle. Vertical lines mark the combustion phases, arrows indicate fuel additions. Top panel: measured mass concentrations accounting for dilution. Due to the constant flow rate through the stove, these are proportional to emissions in μg/s. Middle panel: modified combustion efficiency (MCE). Bottom panel: flue gas O_2 and CO content. Note the different y-axes: PAHs, MCE, and CO on the left axes, OA and O_2 on the right axes.

decreases almost monotonically with increasing m/z. This enables detection of high mass PAH peaks of low abundances. For the two cases presented here, 8−9% of the PAH signal is above m/z 305, corresponding to PAHs with more than 24 carbon atoms (C > 24).

The data clearly show the presence of PAHs of molecular weight up to ∼600 Da, that is, up to C48. These large PAHs warrant further investigation, as literature data is scarce owing to the technical difficulties of measuring them.[25] The relationship between AMS data and actual distribution of such large PAH molecules also require further study. Since heavier PAHs are less volatile, it is conceivable that some large PAHs may not be fully vaporized by the AMS. This can be investigated by comparing results from the AMS (flash vaporization at 600 °C) and the Soot Particle AMS[26] that utilizes a 1064 nm laser for volatilization.

Generally, C16−C18 PAHs have four rings, C20−C22 five, and C24 six. The fuel addition phase was dominated by C16−C19 PAHs, particularly C16 (see Figure 5a). The distribution observed during the intermediate phase was shifted toward larger PAHs, with roughly equal amounts of C16, C18, and C20. The PAH carbon number distribution was similar for the two burn rates in the wood stove at a given combustion phase. The pellet stove operation with reduced air supply produced a distribution similar to the intermediate phase of wood stove combustion. The higher fraction of lighter PAHs during the fuel addition phase may be due to the lower combustion temperature, but it may also be due to increased partitioning into the condensed phase of lighter, more volatile PAHs during the high OA mass loadings occurring. The mass spectra from which Figure 5a was deduced are presented in SI Figure S3.

Figure 5b shows a comparison between measured abundances of C16−C24 PAHs (202−302 Da) by off-line GC-MS and AMS for an intermediate phase at NB. The comparison has been limited to this range due to complexities in assigning the AMS signals below C16 and due to lack of GC-MS data above C24. As the GC-MS data indicates <10% of the particulate PAHs were below C16 while the AMS results imply <10% were above C24. Thus, this comparison encompasses the
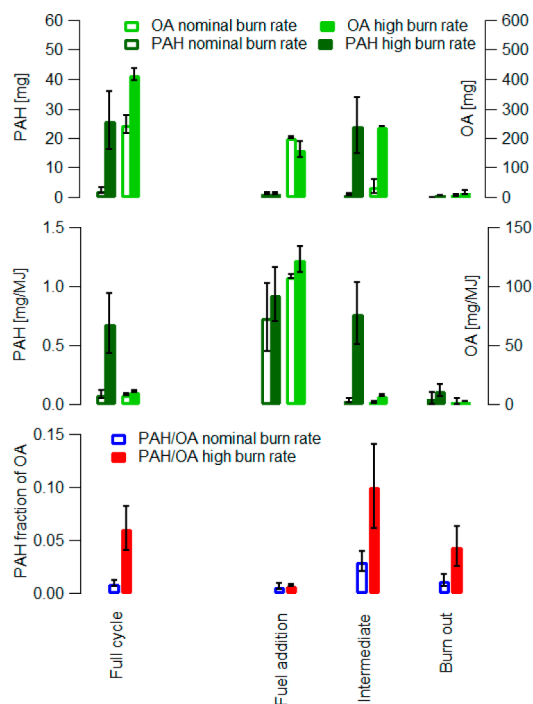
Figure 2. Average wood stove particulate emissions at nominal and high burn rates in mg and mg/MJ for the three combustion phases and the full cycle. Error bars represent range of observations ($n = 2$). The data are also listed in SI Table S2.

majority of the distribution. In general good agreement was found, however a slightly lower mass fraction for C20 (m/z 250−252) for the AMS was found for other samples as well, for unknown reasons. A list of individual PAHs measured with GC-MS and their mass contributions is presented in SI Table S3.

Particle Size Resolved Analysis and Mixing State of Emissions. Particle size-resolved analysis gives insight into the mixing state of particles in a given combustion phase. Size resolved chemical composition can also serve as a signature to apportion biomass combustion particles in ambient air. Figure 6
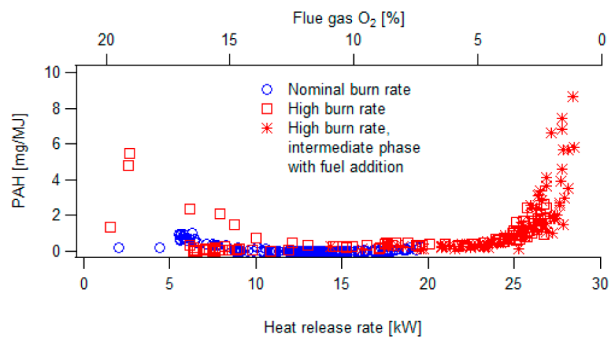
Figure 3. Particulate phase PAH emissions vs measured O_2 concentration and estimated heat release rate for the wood stove. Note the strong increase in PAH emissions at heat release rates above 23 kW (overload with $O_2 < 5\%$) in this combustion system. The elevated PAH emissions at very low heat release rates are associated with addition of fuel on glowing embers.
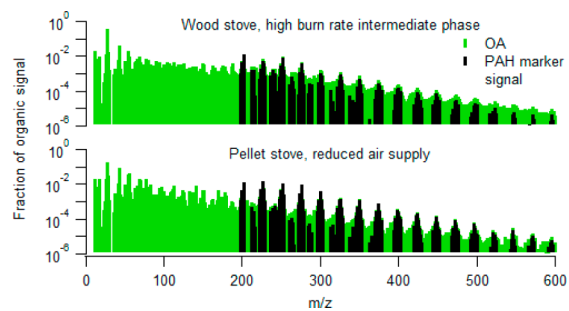

Figure 4. Normalized organic mass spectra from wood stove intermediate phase and artificially degraded, reduced air supply pellet combustion. The most abundant m/z is 28, tentatively attributed to CO^+ (see SI Figure S2). Note the logarithmic y-axes.
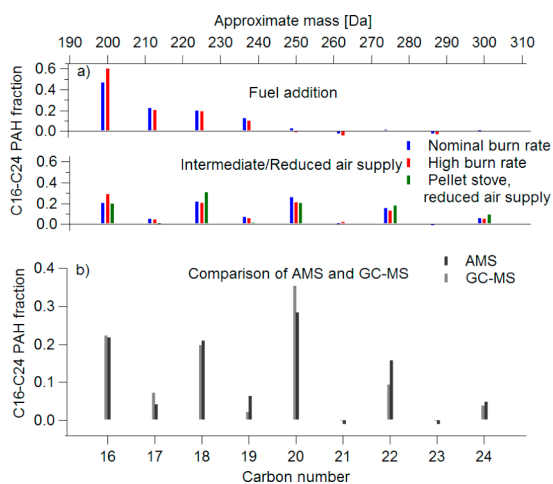
Figure 5. a) PAH carbon number distributions between C16 and C24 (>80% of the total distribution) for fuel addition (top) and intermediate (bottom) phases in the wood stove. Bottom panel also features pellet combustion with reduced air supply. b) Comparison of carbon number distributions of C16−C24 PAHs determined with AMS and GC-MS (collected at the same dilution ratio). Data from a 30 min period of the intermediate phase of a NB wood stove experiment.

shows that particles emitted upon addition of fuel on glowing embers have a relatively large vacuum aerodynamic particle diameter (D_{va}, equivalent diameter based on inertial and drag forces under low pressure[27]): $D_{va} = 600-700$ nm, similar to
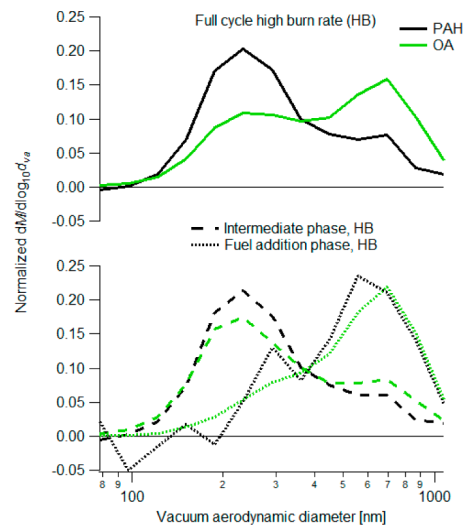
Figure 6. Vacuum aerodynamic size distribution of PAH and OA for a high burn rate cycle. Top: full cycle. Bottom: Fuel addition and intermediate phases. Each distribution is normalized.

heavily aged particles in the atmosphere.[28] During the intermediate phase much smaller particles are emitted (D_{va} ~200 nm). The batch average size distribution at HB is thus bimodal, with OA slightly more abundant in the larger sized mode. PAHs by contrast are emitted predominantly in the smaller mode, as can be expected due to their higher emissions at high heat release rates. This is also consistent with the findings of Hays et al.[29], who observed PAHs shifted to smaller particle sizes compared with total PM in wood stove emissions using a cascade impactor. Furthermore, these authors found an inverse relation between PAH molecular weight and particle size, which can be explained by the shift toward smaller PAHs (Figure 5) and larger particles (Figure 6) during the fuel addition phase. For NB (not shown) the full batch size distribution was similar to the fuel addition phase observed at HB, which is not surprising given that the emissions (OA and PAH) mostly occur during that phase.

The observations of a bimodal, partly externally mixed size distribution are similar to what Pagels, et al.[30] found for batch averaged emissions from a modern wood stove using single particle mass spectrometry. Variations in aerodynamic peak sizes with combustion conditions have also been observed previously in impactor samples for "start" and "intermediate" phases[9] and between hot and cold combustion cases[31] for the full batch. The previous studies that used impactors typically found a unimodal batch average distribution, while our study and Pagels and co-workers found bimodal size distributions. The difference is likely attributed in part to the measurement techniques employed. In aerodynamic equivalent diameter, nonspherical particles (for instance agglomerates such as soot particles) are small compared with spheres of the same mass.[27] This effect is stronger at lower pressures, that is, more pronounced when measured with online mass spectrometry compared with impactor samples. The smaller mode observed in the intermediate phase is likely soot agglomerates, which is why the two modes are more separated in D_{va}.

Full cycle, total PM emissions measured in separate experiments at similar combustion conditions showed ~40 mg/MJ for NB and ~80 mg/MJ for HB, to be compared with organic emissions (incl. PAHs) of 8 mg/MJ (NB) and 11 mg/MJ (HB) from AMS. Thermal-optical analysis (see SI) for

elemental carbon (EC) and organic carbon (OC) was carried out for select experiments. It showed that the EC/OC ratio was 0.1 during the fuel addition phase at HB, whereas it was 3.5 for a full HB cycle and 9 during the hot air starved conditions in the pellet stove. Thus, it is reasonable to assume that most EC emissions will be coemitted with PAHs during hot air starved conditions in the smaller sized mode. The fuel addition phase yields organically dominated particles with larger D_{va}. However, the mixing characteristics of EC with OC, PAHs, and other components require further study. The D_{va} size in the intermediate phase is larger compared to fresh diesel emissions ($D_{va} \sim 100$ nm) which is consistent with agglomerates that are more compact and/or consist of a higher fraction of condensed organics and alkali salts, leading to an increased D_{va}.[30]

PAH and OA Formation Mechanism. It has been shown previously that PAHs form in large quantities and may be emitted under high temperature air-starved wood combustion conditions.[9,32−35] This study illustrates that PAHs can also form during a few minutes following addition of fuel on glowing embers in a wood stove at lower temperatures (400−500 °C), and that the fraction of PAHs with five rings or more increases with increasing temperature. It cannot be ruled out that this is because of gas/particulate partitioning differences, as the lower temperatures coincided with more concentrated organic emissions. In gasification research[36,37] (the study of thermal degradation in the absence of oxygen) one typically distinguishes between primary tars that consist of primary pyrolysis products of cellulose and lignin such as monosaccharide anhydrides (e.g., levoglucosan), and methoxyphenols formed at low temperatures. As the combustion temperature increases these are further broken down to phenols (600−700 °C) and methylated aromatics (>700 °C). At even higher temperatures, the yields of PAHs increase strongly. At such high temperatures, PAHs are also one of the few classes of organic compounds that are stable enough to survive. Based on this reasoning we can understand the strongly increasing PAH/OA ratio and decreased concentration of OA for the intermediate phase of HB compared to the fuel addition phase. Gasification theory also predicts that EC formation and emission increases as the temperature is further increased above the optimal temperature window for PAH formation.

Comparison with Literature Data and Implications for Targeted Emission Control. In this study, we found substantially higher PAH emissions for high burn rate cycles: 0.7 mg/MJ (13 mg/kg dry fuel); compared to nominal burn rate: 0.1 mg/MJ (1.5 mg/kg dry fuel). Orasche et al.[10,33] found that the full batch averaged PAH emissions varied over 2 orders of magnitude for the wood stove systems and fuels investigated. By far, the highest particle phase PAH emissions were found for "overload conditions" (i.e., excessive heat release rates) ∼6 mg/MJ. Their optimal wood stove combustion condition resulted in an emission factor of 0.1 mg/MJ. As comparison, Pettersson et al.[9] studied emissions from the same type of wood stove as used in our study and the particulate PAH emissions were in the range of 0.2−10 mg/MJ, with the highest emissions determined for extreme hot air starved conditions.

In terms of PAH fraction of total particulate mass, we found full batch average values of about 0.2% at nominal burn rate and 1% for high burn rate. Orasche et al.[33] report approximately 0.3% and 10% for the two cases discussed above.

In this study we found a high repeatability of the emissions in the fuel addition phase, whereas in some of our other campaigns it has been more variable from cycle to cycle.

Thus, the OA and PAH emissions upon fuel addition may be strongly variable between users and combustion systems. It is also unclear if such emissions are further enhanced during low temperature burning conditions, for example in open fireplaces and during cold start kindling conditions in wood stoves. Measurements at such conditions could also elucidate whether there are general relationships, for example, between emitted PAHs and CO and O_2. Also, it is unclear how much partitioning effects may lead to an overestimation of particulate PAH emissions during the slow burning pyrolysis, when sampled OA mass loadings are well above ambient concentrations. We note that such effects will always be present when using a method based on a constant flue gas dilution ratio, as was used here, which is common practice in these types of emission studies.

In summary, previous data also supports that PAH emissions from wood stoves can be strongly elevated at air starved combustion conditions at high heat release rates, even more so than found in this study. The most efficient way of reducing PAH emissions from wood stoves may therefore be to target combustion conditions with too high heat release rates that result in air deficits related to the functionality of the specific stove. In our study, fast burning conditions with less than 5% O_2 in the flue gases, corresponding to heat release rates of more than 23 kW, were shown to coincide with increased PAH emissions. While the numbers are stove specific, this phenomenon is (qualitatively) likely not.

Measures to avoid these situations may potentially reduce adverse effects on human health and possibly also have the cobenefit, from a climate warming perspective, of reducing black carbon emissions. Furthermore, emissions of the potent greenhouse gas methane are also enhanced during this kind of intense incomplete combustion.[9] The traditional recommendations to wood stove and boiler users and manufacturers are to avoid slow, low temperature combustion (i.e., moist fuel and poor insulation). Our study illustrates how excessively high heat release rates are also undesirable, because of the emissions of particulate PAHs. It will be a challenge to reformulate and communicate general wood burning guidelines that also include recommendations to avoid air starved combustion conditions.

■ ASSOCIATED CONTENT

⑤ Supporting Information
Description of fuel and combustion characteristics, sampling setup, AMS operation and data analysis, off-line PAH analysis, calculation of emissions with uncertainty estimate, controlled generation of PAHs in the pellet stove, summary of emissions and PAH molecular mass and carbon number distributions. This material is available free of charge via the Internet at http://pubs.acs.org.

■ AUTHOR INFORMATION

Corresponding Author
*Phone: ++4646 2229519; fax: ++4646 2224431; e-mail: Axel.Eriksson@nuclear.lu.se.

Notes
The authors declare no competing financial interest.

■ ACKNOWLEDGMENTS

■ REFERENCES

(1) Bolling, A. K.; Pagels, J.; Yttri, K. E.; Barregard, L.; Sallsten, G.; Schwarze, P. E.; Boman, C., Health effects of residential wood smoke particles: The importance of combustion conditions and physicochemical particle properties. *Part. Fibre Toxicol.* **2009**, *6*.

(2) Naeher, L. P.; Brauer, M.; Lipsett, M.; Zelikoff, J. T.; Simpson, C. D.; Koenig, J. Q.; Smith, K. R. Woodsmoke health effects: A review. *Inhalation Toxicol.* **2007**, *19* (1), 67−106.

(3) Sehlstedt, M.; Dove, R.; Boman, C.; Pagels, J.; Swietlicki, E.; Londahl, J.; Westerholm, R.; Bosson, J.; Barath, S.; Behndig, A. F.; Pourazar, J.; Sandstrom, T.; Mudway, I. S.; Blomberg, A., Antioxidant airway responses following experimental exposure to wood smoke in man. *Part. Fibre Toxicol.* **2010**, *7*.

(4) Boman, C.; Nordin, A.; Thaning, L. Effects of increased biomass pellet combustion on ambient air quality in residential areas - a parametric dispersion modeling study. *Biomass Bioenergy* **2003**, *24* (6), 465−474.

(5) Tapanainen, M.; Jalava, P. I.; Maki-Paakkanen, J.; Hakulinen, P.; Lamberg, H.; Ruusunen, J.; Tissari, J.; Jokiniemi, J.; Hirvonen, M. R. Efficiency of log wood combustion affects the toxicological and chemical properties of emission particles. *Inhalation Toxicol.* **2012**, *24* (6), 343−355.

(6) IARC monographs on the evaluation of carcinogenic risks to humans. *IARC Monogr. Eval. Carcinog. Risks Hum.* **2010**, *95*, 9−38.

(7) Poulain, L.; Iinuma, Y.; Muller, K.; Birmili, W.; Weinhold, K.; Bruggemann, E.; Gnauk, T.; Hausmann, A.; Loschau, G.; Wiedensohler, A.; Herrmann, H. Diurnal variations of ambient particulate wood burning emissions and their contribution to the concentration of polycyclic aromatic hydrocarbons (PAHs) in Seiffen, Germany. *Atmos Chem. Phys.* **2011**, *11* (24), 12697−12713.

(8) Lamberg, H.; Nuutinen, K.; Tissari, J.; Ruusunen, J.; Yli-Pirila, P.; Sippula, O.; Tapanainen, M.; Jalava, P.; Makkonen, U.; Teinila, K.; Saarnio, K.; Hillamo, R.; Hirvonen, M. R.; Jokiniemi, J. Physicochemical characterization of fine particles from small-scale wood combustion. *Atmos. Environ.* **2011**, *45* (40), 7635−7643.

(9) Pettersson, E.; Boman, C.; Westerholm, R.; Bostrom, D.; Nordin, A. Stove performance and emission characteristics in residential wood log and pellet combustion, part 2: Wood stove. *Energ Fuel* **2011**, *25*, 315−323.

(10) Orasche, J.; Seidel, T.; Hartmann, H.; Schnelle-Kreis, J.; Chow, J. C.; Ruppert, H.; Zimmermann, R. Comparison of emissions from wood combustion. Part 1: Emission factors and characteristics from different small-scale residential heating appliances considering particulate matter and polycyclic aromatic hydrocarbon (PAH)-related toxicological potential of particle-bound organic species. *Energy Fuel* **2012**, *26* (11), 6695−6704.

(11) Boman, C.; Nordin, A.; Westerholm, R.; Pettersson, E. Evaluation of a constant volume sampling setup for residential biomass fired appliances—Influence of dilution conditions on particulate and PAH emissions. *Biomass Bioenergy* **2005**, *29* (4), 258−268.

(12) Hedberg, E.; Kristensson, A.; Ohlsson, M.; Johansson, C.; Johansson, P. A.; Swietlicki, E.; Vesely, V.; Wideqvist, U.; Westerholm, R. Chemical and physical characterization of emissions from birch wood combustion in a wood stove. *Atmos. Environ.* **2002**, *36* (30), 4823−4837.

(13) Lillieblad, L.; Szpila, A.; Strand, M.; Pagels, J.; Rupar-Gadd, K.; Gudmundsson, A.; Swietlicki, E.; Bohgard, M.; Sanati, M. Boiler operation influence on the emissions of submicrometer-sized particles and polycyclic aromatic hydrocarbons from biomass-fired grate boilers. *Energy Fuel* **2004**, *18* (2), 410−417.

(14) Heringa, M. F.; DeCarlo, P. F.; Chirico, R.; Lauber, A.; Doberer, A.; Good, J.; Nussbaumer, T.; Keller, A.; Burtscher, H.; Richard, A.; Miljevic, B.; Prevot, A. S. H.; Baltensperger, U. Time-resolved characterization of primary emissions from residential wood combustion appliances. *Environ. Sci. Technol.* **2012**, *46* (20), 11418−11425.

(15) Dzepina, K.; Arey, J.; Marr, L. C.; Worsnop, D. R.; Salcedo, D.; Zhang, Q.; Onasch, T. B.; Molina, L. T.; Molina, M. J.; Jimenez, J. L.

Detection of particle-phase polycyclic aromatic hydrocarbons in Mexico City using an aerosol mass spectrometer. *Int. J. Mass Spectrom.* **2007**, *263* (2−3), 152−170.

(16) Marr, L. C.; Dzepina, K.; Jimenez, J. L.; Reisen, F.; Bethel, H. L.; Arey, J.; Gaffney, J. S.; Marley, N. A.; Molina, L. T.; Molina, M. J. Sources and transformations of particle-bound polycyclic aromatic hydrocarbons in Mexico City. *Atmos. Chem. Phys.* **2006**, *6*, 1733−1745.

(17) Weimer, S.; Alfarra, M. R.; Schreiber, D.; Mohr, M.; Prevot, A. S. H.; Baltensperger, U., Organic aerosol mass spectral signatures from wood-burning emissions: Influence of burning conditions and wood type. *J. Geophys. Res.: Atmos.* **2008**, *113*, (D10).

(18) Elsasser, M.; Busch, C.; Orasche, J.; Schon, C.; Hartmann, H.; Schnelle-Kreis, J.; Zimmermann, R. Dynamic changes of the aerosol composition and concentration during different burning phases of wood combustion. *Energy Fuel* **2013**, *27* (8), 4959−4968.

(19) Lyyranen, J.; Jokiniemi, J.; Kauppinen, E. I.; Backman, U.; Vesala, H. Comparison of different dilution methods for measuring diesel particle emissions. *Aerosol Sci. Technol.* **2004**, *38* (1), 12−23.

(20) Robinson, A. L.; Donahue, N. M.; Shrivastava, M. K.; Weitkamp, E. A.; Sage, A. M.; Grieshop, A. P.; Lane, T. E.; Pierce, J. R.; Pandis, S. N. Rethinking organic aerosols: Semivolatile emissions and photochemical aging. *Science* **2007**, *315* (5816), 1259−1262.

(21) DeCarlo, P. F.; Kimmel, J. R.; Trimborn, A.; Northway, M. J.; Jayne, J. T.; Aiken, A. C.; Gonin, M.; Fuhrer, K.; Horvath, T.; Docherty, K. S.; Worsnop, D. R.; Jimenez, J. L. Field-deployable, high-resolution, time-of-flight aerosol mass spectrometer. *Anal. Chem.* **2006**, *78* (24), 8281−8289.

(22) Paloposki, T.; Saastamoinen, J.; Klobut, K.; Tuomaala, P. Analysis of wood firing in stoves by the oxygen consumption method and the carbon dioxide generation method. *Biomass Bioenergy* **2014**, *61*, 1−24, DOI: 10.1016/j.biombioe.2011.12.041.

(23) Londahl, J.; Pagels, J.; Boman, C.; Swietlicki, E.; Massling, A.; Rissler, J.; Blomberg, A.; Bohgard, M.; Sandstrom, T. Deposition of biomass combustion aerosol particles in the human respiratory tract. *Inhalation Toxicol.* **2008**, *20* (10), 923−933.

(24) Pagels, J.; Strand, M.; Rissler, J.; Szpila, A.; Gudmundsson, A.; Bohgard, M.; Lillieblad, L.; Sanati, M.; Swietlicki, E. Characteristics of aerosol particles formed during grate combustion of moist forest residue. *J. Aerosol Sci.* **2003**, *34* (8), 1043−1059.

(25) Bergvall, C.; Westerholm, R. Determination of 252−302 Da and tentative identification of 316−376 Da polycyclic aromatic hydrocarbons in Standard Reference Materials 1649a Urban Dust and 1650b and 2975 Diesel Particulate Matter by accelerated solvent extraction−HPLC-GC-MS. *Anal. Bioanal. Chem.* **2008**, *391*, 2235−2248.

(26) Onasch, T. B.; Trimborn, A.; Fortner, E. C.; Jayne, J. T.; Kok, G. L.; Williams, L. R.; Davidovits, P.; Worsnop, D. R. Soot particle aerosol mass spectrometer: Development, validation, and initial application. *Aerosol Sci. Technol.* **2012**, *46* (7), 804−817.

(27) DeCarlo, P. F.; Slowik, J. G.; Worsnop, D. R.; Davidovits, P.; Jimenez, J. L. Particle morphology and density characterization by combined mobility and aerodynamic diameter measurements. Part 1: Theory. *Aerosol Sci. Technol.* **2004**, *38* (12), 1185−1205.

(28) Massoli, P.; Fortner, E. C.; Canagaratna, M. R.; Williams, L. R.; Zhang, Q.; Sun, Y.; Schwab, J. J.; Trimborn, A.; Onasch, T. B.; Demerjian, K. L.; Kolb, C. E.; Worsnop, D. R.; Jayne, J. T. Pollution gradients and chemical characterization of particulate matter from vehicular traffic near major roadways: Results from the 2009 Queens College Air Quality Study in NYC. *Aerosol Sci. Technol.* **2012**, *46* (11), 1201−1218.

(29) Hays, M. D.; Smith, N. D.; Kinsey, J.; Dong, Y.; Kariher, P. Polycyclic aromatic hydrocarbon size distributions in aerosols from appliances of residential wood combustion as determined by direct thermal desorption-GCMS. *J. Aerosol Sci.* **2003**, *34* (8), 1061−108.

(30) Pagels, J.; Dutcher, D. D.; Stolzenburg, M. R.; McMurry, P. H.; Galli, M. E.; Gross, D. S. Fine-particle emissions from solid biofuel combustion studied with single-particle mass spectrometry: Identification of markers for organics, soot, and ash components. *J. Geophys. Res.: Atmos.* **2013**, *118* (2), 859−870.

(31) Rau, J. A. Composition and size distribution of residential wood smoke particles. *Aerosol Sci. Technol.* **1989**, *10* (1), 181−192.

(32) Hytonen, K.; Yli-Pirila, P.; Tissari, J.; Grohn, A.; Riipinen, I.; Lehtinen, K. E. J.; Jokiniemi, J. Gas-particle distribution of PAHs in wood combustion emission determined with annular denuders, filter, and polyurethane foam adsorbent. *Aerosol Sci. Technol.* **2009**, *43* (5), 442−454.

(33) Orasche, J.; Schnelle-Kreis, J.; Schon, C.; Hartmann, H.; Ruppert, H.; Arteaga-Salas, J. M.; Zimmermann, R. Comparison of emissions from wood combustion. Part 2: Impact of combustion conditions on emission factors and characteristics of particle-bound organic species and polycyclic aromatic hydrocarbon (PAH)-related toxicological potential. *Energy Fuel* **2013**, *27* (3), 1482−1491.

(34) McDonald, J. D.; Zielinska, B.; Fujita, E. M.; Sagebiel, J. C.; Chow, J. C.; Watson, J. G. Fine particle and gaseous emission rates from residential wood combustion. *Environ. Sci. Technol.* **2000**, *34* (11), 2080−2091.

(35) Fine, P. M.; Cass, G. R.; Simoneit, B. R. T. Chemical characterization of fine particle emissions from fireplace combustion of woods grown in the northeastern United States. *Environ. Sci. Technol.* **2001**, *35* (13), 2665−2675.

(36) Milne, T. A.; Evans, R. J.; Abatzoglou, N. *Biomass Gasifier "Tars": Their Nature, Formation and Conversion*, NREL/TP-570-25357; National Renewable Energy Laboratory, **1998**. .

(37) Li, C. S.; Suzuki, K. Tar property, analysis, reforming mechanism and model for biomass gasification—An overview. *Renewable Sustainable Energy Rev.* **2009**, *13* (3), 594−604.